Colloids and Surfaces B: Biointerfaces 221 (2023) 112968

Contents lists available at ScienceDirect

Colloids and Surfaces B: Biointerfaces

journal homepage: www.elsevier.com/locate/colsurfb

On the uptake of cationic liposomes by cells: From changes in elasticity to internalization

Adrià Botet-Carreras [a,b], Manel Bosch Marimon [c,d], Ruben Millan-Solsona [e,f], Eva Aubets [g], Carlos J. Ciudad [b,g], Véronique Noé [b,g], M. Teresa Montero [a,b], Òscar Domènech [a,b,*], Jordi H. Borrell [a]

[a] Secció de Fisicoquímica, Facultat de Farmàcia i Ciències de l'Alimentació,Universitat de Barcelona (UB), 08028 Barcelona, Catalonia, Spain
[b] Institute of Nanoscience and Nanotechnology (IN2UB),Universitat de Barcelona (UB), 08028 Barcelona, Catalonia, Spain
[c] Unitat de Microscòpia Òptica Avançada, Centres Científics i Tecnològics (CCiTUB),Universitat de Barcelona (UB), 08028 Barcelona, Catalonia, Spain
[d] Departament de Bioquímica i Biomedicina Molecular, Facultat de Biologia,Universitat de Barcelona (UB), 08028 Barcelona, Catalonia, Spain
[e] Nanoscale Bioelectrical Characterization, Institute for Bioengineering of Catalonia (IBEC), The Barcelona Institute of Science and Technology (BIST),Universitat de Barcelona (UB), 08028 Barcelona, Catalonia, Spain
[f] Departament d'Enginyeria Electrònica i Biomèdica,Facultat de Física,Universitat de Barcelona (UB), 08028 Barcelona, Catalonia, Spain
[g] Departament de Bioquímica i Fisiologia, Facultat de Farmàcia i Ciències de l'Alimentació, Universitat de Barcelona (UB), 08028 Barcelona, Catalonia, Spain

ARTICLE INFO

Keywords:
Engineered liposomes
Drug delivery system
Atomic force microscopy
Young's modulus
Confocal microscopy
Filopodia

ABSTRACT

In this study, we assessed the capacity of a previously reported engineered liposomal formulation, which had been tested against model membranes mimicking the lipid composition of the HeLa plasma membrane, to fuse and function as a nanocarrier in cells. We used atomic force microscopy to observe physicochemical changes on the cell surface and confocal microscopy to determine how the liposomes interact with cell membranes and released their load. In addition, we performed viability assays using methotrexate as an active drug to obtain proof of concept of the formulation's capacity to function as a drug delivery-system. The interaction of engineered liposomes with living cells corroborates the information obtained using model membranes and supports the capacity of the engineered liposomal formulation to serve as a potential nanocarrier.

1. Introduction

Ever since the first observations were reported in the 1960s, liposomes have been regarded either as model membranes or as drug delivery systems [1]. In the case of the latter, several engineered formulations based on liposomes have emerged in the market as successful anticancer agents [2]. In addition to a phospholipid matrix, most of the available liposome formulations include polyethylene glycol, earlier recognized as a fusogenic agent [3], which enhances target efficiency and activity [4,5]. This is a crucial point because liposome activity in cancer treatment and other therapeutic uses may be efficient when applied to cell cultures, but may often fail when administered to animal models. Even immunoliposomes can be specific against cells in culture but unsuccessful for specific targeting when injected into the blood stream [6–8]. Despite all the drawbacks encountered over the years, several liposome formulations have reached the market [9]. At present, decorated liposomes and surface-engineered liposomes have emerged as a promising strategy in drug delivery systems [10].

Besides formulation strategies, one of the questions that remain unsolved is how rough lipid-based liposomes interact with cell membranes and which of the basic mechanisms, such as adsorption, fusion, endocytosis, or perhaps a combination of them, are involved in liposome internalization by cells. Liposome-cell membrane interactions can be extremely different depending on the nature of the cell membrane (lipid composition and structure) and liposome lipid composition. All these aspects have been reviewed widely elsewhere [11]. In principle, liposome internalization may be promoted by including specific lipids that enhance recognition in the bilayer membrane of the target cell. In this regard, it is known that cholesterol (CHOL) and cationic liposomes containing positively-charged lipids enhance fusion with the cell membrane and thus promote subsequent internalization [12]. Liposome-cell interactions are dependent on the composition, structure, and dynamics

* Correspondence to: Physical Chemistry Section, Dept. of Pharmacy and Pharmaceutical Technology and Physical Chemistry, Faculty of Pharmacy and Food Sciences, University of Barcelona, Avda. Joan XXIII, 27-31, 08028 Barcelona, Spain.
E-mail address: odomenech@ub.edu (Ò. Domènech).

https://doi.org/10.1016/j.colsurfb.2022.112968
Received 2 May 2022; Received in revised form 14 October 2022; Accepted 22 October 2022
Available online 26 October 2022

of each cell membrane. In brief, a variety of biophysical methods have been applied over the years to investigate the fusion mechanism or/and effectiveness of drug delivery by using membrane models with a specific lipid composition [13].

In an earlier study we investigated the fusion mechanism of liposomes using a simplified model of the HeLa membrane that mimicked the cell lipid membrane [14]. We showed that liposomes formed with 1-palmitoyl-2-oleoyl-phosphatidylcholine (POPC), 1,2-dioleoyl-3-trimethylammonium-propane (DOTAP) and CHOL (0.80:0.20, mol/mol), at a molar ratio POPC:CHOL:DOTAP (0.65:0.15:0.20, mol/mol/mol) fuse with lipid monolayers and liposomes mimicking the HeLa cell lipid membrane. In that report, we hypothesized a possible mechanism involving adsorption and insertion of the phospholipids into the lipid model used. These studies suggested the involvement of adhesion forces throughout the entire fusion process [15]. This physicochemical magnitude may be implicated not only in the membrane-membrane fusion but also in the uptake mechanism of liposomes into cells. However, the membrane of living HeLa cells is much more complex than the model investigated earlier. For this reason, in the present study we took the next step forward to obtain a better insight into the mechanism of interaction of the engineered liposomes that positively fuse with the lipid HeLa model, this time using live HeLa cells.

In the present study we focus our aim on how the interaction of liposomes of a previously investigated lipid composition [14,16] could modulate the physicochemical properties of HeLa cells and whether they can be used as drug nanocarriers. To this end, we used atomic force microscopy (AFM) and confocal microscopy (CM) to study how the interaction of POPC:DOTAP:CHOL liposomes with HeLa cells affects membrane nanomechanics properties of the cell and the eventual internalization of liposomes. Since flow cytometry can observe the presence of liposomes in the cell but it cannot discriminate between liposome adsorption, fusion, or association in the cells, we further investigated the incorporation of liposomes into HeLa cytoplasm by means of CM. With this objective, we engineered liposomes encapsulating calcein at a self-quenching concentration and labeled at the bilayer level with Rh-PE, and after incubation with HeLa cells, we observed the release of calcein into the cytoplasm. We also investigated possible correlations between nanomechanical properties and the pharmacological action of engineered liposomes loaded with methotrexate (MTX).

2. Material and methods

2.1. Materials

1-palmitoyl-2-oleoyl-*sn*-glycero-3-phosphatidylcholine (POPC), 1,2-dioleoyl-3-trimethylammonium-propane (chloride salt) (DOTAP) and cholesterol (CHOL) were purchased from Avanti Polar Lipids (Alabaster, AL, USA). 1,2-dioleoyl-*sn*-glycero-3-phosphoethanolamine-N-(lissamine rhodamine B sulfonyl) (Rh-PE) and Cell Mask Deep Red Plasma membrane stain were purchased from ThermoFisher Scientific. Calcein was purchased to Sigma-Aldrich, Madrid, Spain. Fetal bovine serum (FBS) was purchased from Life Technologies, Madrid, Spain. Methotrexate (MTX) was acquired from Pfizer, Madrid. All other reagents were purchased from Merck, Madrid, Spain.

3. Methods

3.1. Preparation of cationic liposomes

Liposomes were prepared as described elsewhere [17]. Briefly, chloroform:methanol (2:1, v/v) solutions containing the appropriate amount of lipids of POPC:CHOL:DOTAP (0.65:0.15:0.20, mol/mol/mol) were placed in a glass balloon flask and dried in a rotary evaporator at room temperature, protected from light. The resulting thin film was kept under high vacuum overnight to remove any traces of organic solvent. Multilamellar liposomes were obtained by redispersion of the thin film in 10 mM Tris·HCl, 150 mM NaCl buffer, pH 7.4. Large unilamellar vesicles were obtained by extrusion through polycarbonate membranes with a pore size of 100 nm, using an Avanti®Mini-extruder (Avanti Polar Lipids Inc., Alabaster, AL, USA). The mean particle size and polydispersity values of the liposomes were measured by dynamic light scattering with a Zetasizer Nano S (Malvern Instruments, UK). To label liposomes with Rh-PE, 0.6 % mol of Rh-PE was added at the initial chloroform:methanol solution of lipids.

To encapsulate calcein for CM experiments a procedure earlier described was used to get the molecule self-quenched into the aqueous space of the liposomes [18]. To this end, liposomes were formed in a buffer containing 103 mM of calcein, extruded, and eluted through a Sephadex G-50 column to separate the free calcein.

3.2. Force volume microscopy AFM and force curves analysis

Force Volume Microscopy is based in acquiring deflection curves at all points of the sample. Later, the post-processing and quantification of the acquired curves enables obtaining topographic, slope, adherence images and Young's module maps. Experiments were performed with a Nanowizard 4 Bio-Atomic Force Microscope, integrated with an inverted optical microscope (Zeiss). The Zeiss microscope was used to visually position the AFM cantilever with respect to the sample. The nanoindentation AFM probes used in this work had 4 μm diameter and nominal spring constant of 0.2 N/m (Nanotools). Before each experiment, the cantilever spring constant was calibrated using the thermal noise method and the photodetector optical sensitivity was determined using a clean Petri dish area as an infinitely rigid substrate. The rate of a single approach-retract cycle was set to 13 Hz and with a resolution of 128 × 128 pixels. During the experiments, the force applied to the samples was kept as low as possible to minimize sample damage. A force threshold was chosen to ensure sample penetration of 0.5–1 μm for all experiments (force threshold = 5 nN).

3.3. Young's modulus determination

Young's modulus was calculated as described elsewhere [19]. The value of this parameter informs on the cohesive forces between the lipids forming the lipid bilayer providing means to unveil changes on a cell membrane [20,21]. To study the cellular process by AFM, the Young's modulus is usually determined as a first approximation by using the Hertz model [22]. If we consider the indenter as a parabolic tip, the Young's modulus can be calculated from force-indentation curve data using

$$F = \frac{4\sqrt{r_{tip}}}{3} \cdot \frac{E}{1-\upsilon^2} \cdot \delta^{3/2} \quad (1)$$

where F is the force from the force curve, r_{tip} is the radius of the spherical punch, δ the indentation, υ the Poisson's ratio (0.5 for most biological samples) and E the Young's modulus.

3.4. Cell culture

HeLa cells were maintained in high glucose DMEM supplemented with 10 % FBS and incubated at 37 °C in a humidified 5 % CO_2 atmosphere.

In the experiments involving the incubation with MTX, cells were incubated in RPMI medium lacking the final products of DHFR activity, hypoxanthine, and thymidine (-HT), and supplemented with 7 % v/v dialyzed FBS.

3.5. Flow cytometry

HeLa cells (50,000) were plated in 6-well dishes the day before

adding the liposomes marked with Rh-PE. After 24 h of incubation with increasing concentration of liposomes (5, 10 or 20 μM), cells were trypsinized and collected, centrifuged at 800 x *g* at 4 ºC for 5 min and washed once in PBS. The pellet was resuspended in 500 μL of PBS and Propidium Iodide was added to a final concentration of 5 μg/mL. Flow cytometry analyses were performed in a FACSAria Fusion System cell sorter (Becton Dickinson, Spain).

3.6. Confocal microscopy and image analyses

For CM observation cells were seeded on glass-bottom dishes. The initial incubation of cells with liposomes (40 μM) was done directly under the microscope in low glucose DMEM without phenol red and with HEPES (10 mM). Incubation with liposomes (20 μM) for 24 h and 48 h was done inside a CO_2 incubator in supplemented DMEM.

Cell membranes were stained using Cell Mask Deep Red Plasma membrane stain. Cells were incubated for 5 min at 37 ºC with Cell Mask (3 μg/mL) diluted in supplemented DMEM. Then cells were washed with prewarmed DPBS and kept in low glucose DMEM without phenol red and with HEPES (10 mM) for fluorescence imaging.

CM images were acquired using a Zeiss LSM 880 confocal microscope equipped with a Heating Insert P S (Pecon) and a 5 % CO_2 providing system. Cells were observed at 37 °C using a 63 × 1.4 NA oil immersion objective. Images were acquired with a voxel size of 0.09 × 0.09 × 0.37 μm (xyz). Calcein, Rhodamine and Cell Mask Deep Red stains were excited with the 488 nm, 561 nm and 633 nm laser lines, respectively.

CM images were analyzed using the Fiji software [23]. Intensity analysis plots were generated with the Multichannel Plot Profile analysis tool of the BAR plugin [24].

3.7. Cell assay viability

Cells (10,000) were plated in 6-well dishes in RPMI medium. Fifteen hours later, liposomes loaded with MTX were added to the culture media. Five days after treatment, 0.63 mM of 3-(4,5-dimetilthyazol-2-yl)− 2,5-diphenyltetrazolium bromide and 100 μM sodium succinate were added to the culture medium and incubated for 2,5 h at 37 °C. After incubation, culture medium was removed and the lysis solution (0.57 % of acetic acid and 10 % of sodium dodecyl sulfate in dimethyl sulfoxide) was added. Absorbance was measured at 570 nm in a Modulus Microplate spectrophotometer (Turner BioSystems). The results were expressed as the percentage of cell survival relative to the controls.

In addition, cell images for each condition were taken using a ZOE Fluorescent Cell Imager (Bio-Rad Laboratories, Inc, Spain) before the MTT assays.

4. Results

We assessed the primary interaction between liposomes and HeLa cells using flow cytometry. Fig. 1 shows the results obtained when HeLa cells were incubated for 24 h with different concentrations of liposomes containing a fluorescent label. Liposomes showed mean diameter size of 117.6 ± 1.1 nm, a polydispersive index of 0.122 and zeta potential mean value of − 8.9 ± 1.1 mV. As can be seen in Fig. 1 A, this approach enabled us to verify whether the liposomes remained on the cell surface or entered the cells. Notably, in Fig. 1B it can be seen that fluorescence intensity increased as the liposome concentration rose.

AFM has evolved from a technique for visualizing samples at high resolution to modes that make possible to obtain physicochemical properties of the samples such as Young's modulus, adhesion forces, or deformation at the nanoscopic level. In the present study, we used AFM to analyze adhesion forces and Young's modulus in HeLa cells before and after the addition of liposomes, and to investigate if these liposomes had been adsorbed, integrated or embedded in the cell membrane by fusion as inferred by biophysical approaches [14,16]. To this end, a spherical punch particle (2 μm) was attached to the sharp tip of the cantilever (Fig. S1A) to minimize any puncturing of the cell lipid membrane and maximize surface interaction in the *sphere-plane geometry* (Fig. S1B). Topographic, adhesion and slope images of a HeLa cell are shown in Fig. 2 before (images A, B and C) and 40 min after the addition of the engineered liposomes (images D, E and F). HeLa cells deposited onto the surface substrate (Fig. 2A) were elliptical structures with mean diameter values ranging from 38 to 45 μm and with average height values of 4–5 μm. The adhesion force values between the tip and the HeLa surface (Fig. 2B) were lower (darker) than with the substrate (Fig. 2E). Interestingly, after the engineered liposomes had been added to the sample, the difference in adhesion force between cell and substrate was reduced. The adhesion force distribution histograms in Figs. 2B and 2E (Figure S2A) show a bimodal distribution of the sample before incorporation of the engineered liposomes, with one peak centered at 2.91 nN, corresponding to the HeLa cell surface, and a second peak centered at 4.33 nN, corresponding to the substrate. Following addition of the engineered liposomes, the distribution became unimodal with a mean adhesion force value of 3.12 nN, and the second peak was

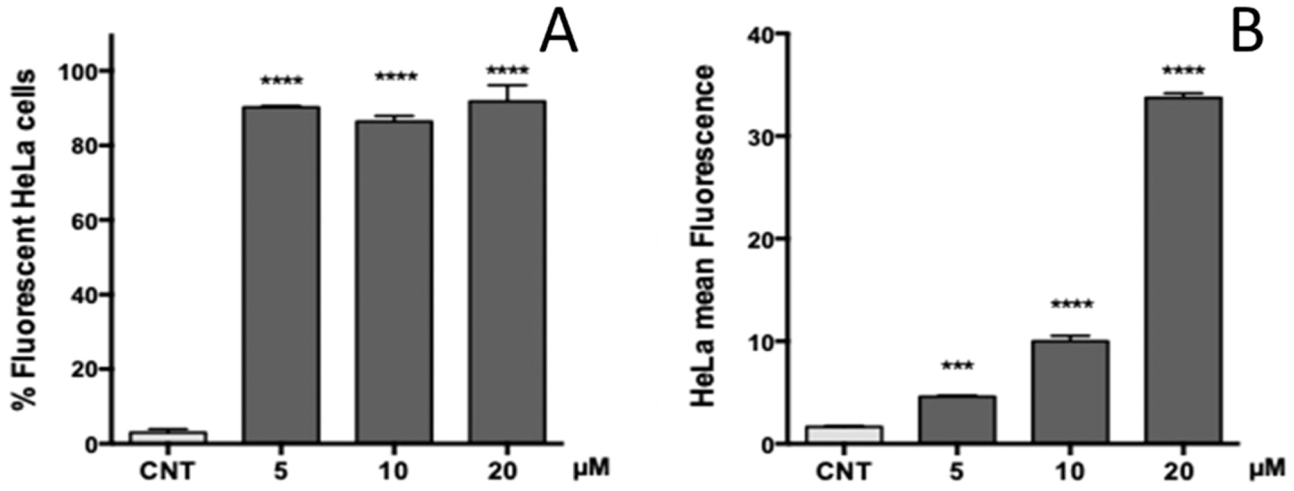

Fig. 1. Flow cytometry assay after 24 h incubation of HeLa cells with engineered liposomes. Percentage of fluorescence (A) and total fluorescence signal as a function of liposome concentration (B). Data are represented as the mean ± SEM of at least three independent experiments. GraphPad Prism version 6.0 software (GraphPad Software, CA, USA) was used. Statistical significance was calculated using one-way ANOVA with Dunnett's multiple comparisons test. Statistical significance levels were denoted as: $p < 0.001$ (***) or $p < 0.0001$ (****).

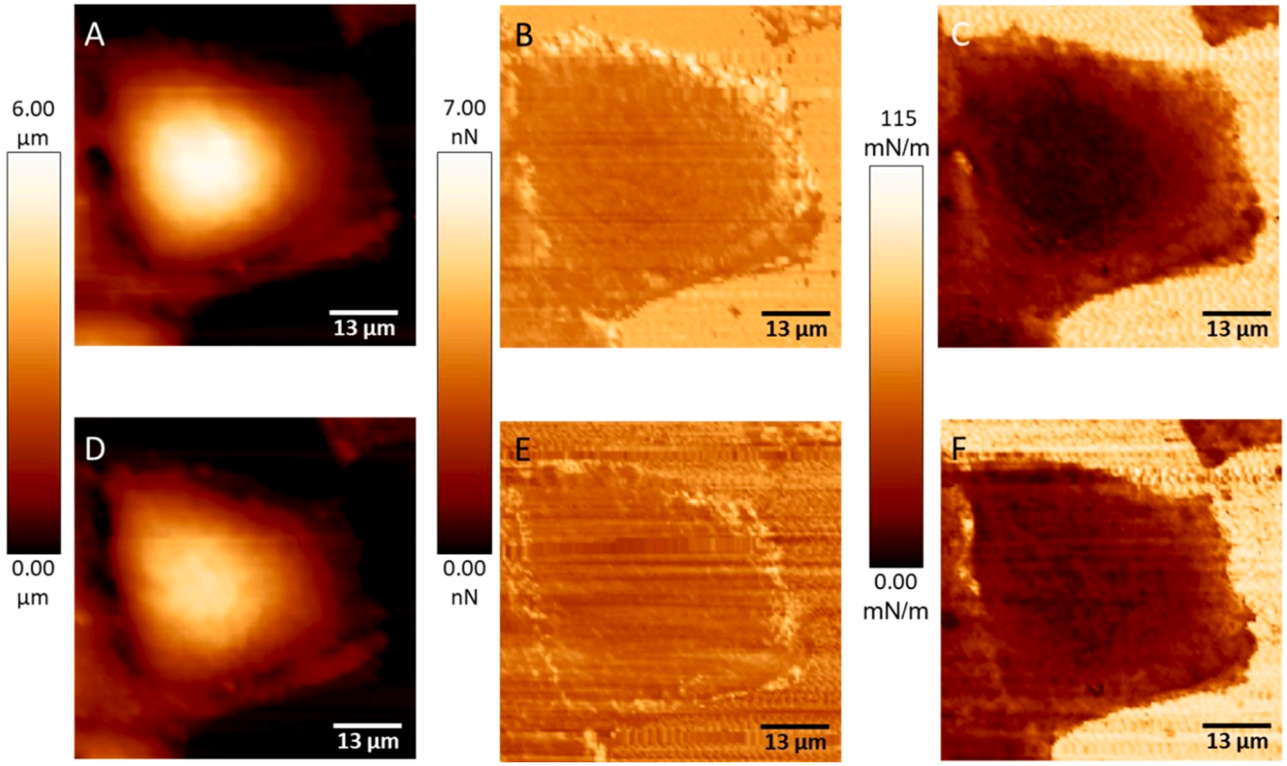

Fig. 2. AFM images of HeLa cells providing different information; Topography (A) and (D); Adhesion (B) and (E); Slope (C) and (F) without the addition of liposomes (A, B, C) or 40 min after liposomes were added (D, E, F).

not observed because the liposomes have been most likely adsorbed onto the modified surface of the substrate. The mean value of the adhesion force after incorporation of the engineered liposomes was slightly higher than the peak attributed to the HeLa cell prior to incorporation. This supports the fact that the liposomes had indeed reached the surface of the HeLa cells.

The slope images shown in Fig. 2C and F provide information about the rigidity of the regions observed. Thus, the higher (brighter) the slope value the greater the rigidity of the sample (Figure S1C). As can be seen in Fig. 2C, the substrate region was much more rigid than the HeLa cell surface, and after incorporation of the liposomes (Fig. 2F) no significant changes were observed either in the HeLa surface or in the substrate.

To obtain further insight in the interaction between the liposomes and the HeLa cells, Young's modulus was determined before and 40 min after the addition of the engineered liposomes. Fig. 3A and B give the elasticity maps of the central region of the HeLa cell shown in Fig. 2A and D, respectively. Higher values (brighter regions) were observed after incorporation of the liposomes. Fig. 3C shows histograms of individual Young's modulus values from Fig. 3A and B. The mean Young's modulus values before and after incorporation of liposomes, calculated by fitting the Gaussian distribution model to the experimental data, were 1.45 ± 0.01 kPa and 2.13 ± 0.02 kPa, respectively.

Although AFM is a suitable technique for visualizing and determining physicochemical parameters of biological samples, it is very

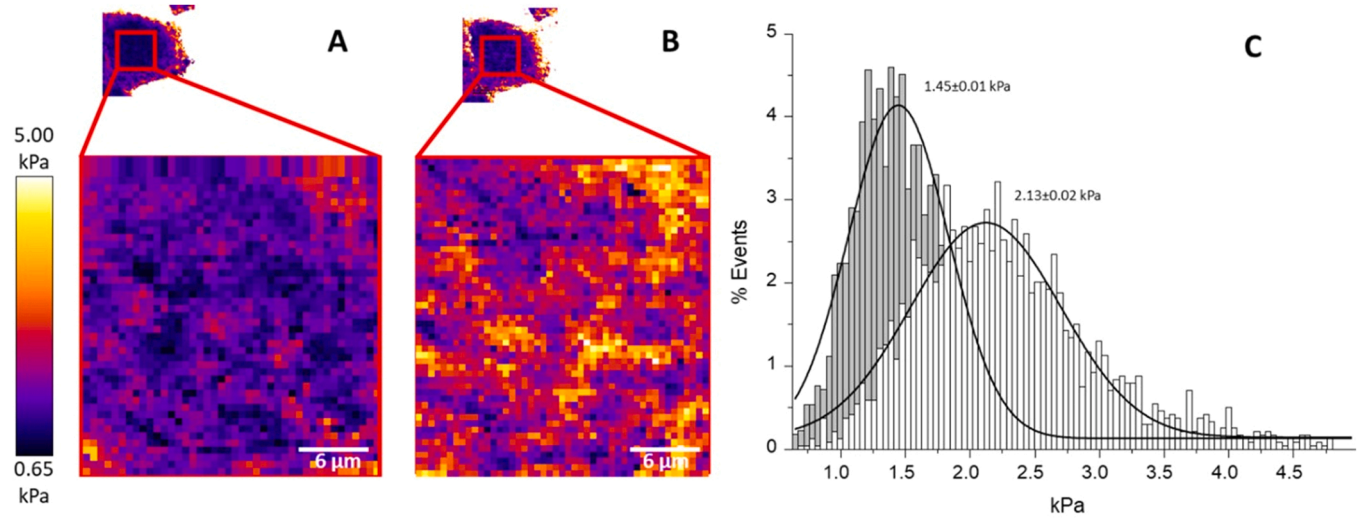

Fig. 3. Force volume of the HeLa cell before (A) and after incubation with engineered liposomes (B). Histogram plot of the force curves on each section A (1.45 kPa) and B (2.13 kPa) (C).

limited as regards identifying the nature of the structures analyzed. Therefore, we further investigated the effect of the engineered liposomes on HeLa cells by means of CM. Thus, we incubated HeLa cells for 40 min with liposomes labelled with Rh-PE and encapsulating calcein at a self-quenching concentration. In addition, HeLa membranes were stained with Cell Mask Deep Red. Fig. 4 shows representative time lapse images from the early distribution of the engineered liposomes after their addition to the HeLa cell culture. Liposomes were quickly adsorbed onto the extracellular membranes and characteristic filopodia of this cell line, these latter becoming an active structure in liposome capture (see video of the kinetic process of interaction of engineered liposomes with HeLa cells, SV1 in *Supplementary Information*). This fast adsorption could be related with the small size of the liposomes due to the fact that small liposomes exhibit high lipid curvature that promotes destabilization when interacting with flat surfaces. As filopodia (white arrows) captured the liposomes, the fluorescence emission of these latter changed from red (PE-Rho fluorescence) to orange, indicating the release of encapsulated calcein from the liposome. Furthermore, when incubation time was increased (Fig. 4B and C) the liposomes began to reach the cell membrane (white arrowheads), either because the filopodia transported them to the membrane or by simple sedimentation from the solution.

Fig. 5 shows the HeLa cells 40 min and 24 h after incubation with the engineered liposomes. At 40 min (Fig. 5A), few liposomes had been internalized into the cell (cyan arrowheads) and they accumulated on the membrane (white arrowheads) or still adhered to filopodia (white arrows). The intensity profile along the yellow line in Fig. 5A indicates that the liposomes emitted both, red and green fluorescence, suggesting that part of the encapsulated calcein was released close to the liposome (Fig. 5B).

After 24 h of incubation (Fig. 5C), most of the liposomes were observed inside the cells and only a few of them were still detected at the membrane level. Interestingly, in Fig. 5C, two liposomes can be seen inside the cell (cyan arrowheads) emitting an orange color with a greenish trail, probably due to the release of calcein during internalization. Fig. 5D shows the intensity profiles along the yellow line in Fig. 5C, where the fluorescence signal after 24 h of incubation was inherent to the Rh-PE fluorescence with almost no calcein signal. Unexpectedly, in other cells, the liposomes presented high calcein intensity close to the PE-Rho fluorescence signal (Fig. 5E), indicating that calcein remained close to the lipid membrane of the liposome. Noteworthily, many liposomes with high green signal were observed at the leading edge of the cells (cyan arrow) suggesting an interaction of the migrating cell with the liposomes attached to the extracellular matrix. The lack of a calcein fluorescence signal in some cells may have been attributed to various reasons: i) calcein was released and distributed throughout the entire cell as a result of incubation time probably by fusion with the membrane; or ii) liposomes were endocytosed and calcein remain self-quenched.

A proof of concept was required to demonstrate that the engineered liposomes could be useful as drug delivery systems. To this end, MTX was encapsulated in the liposomes, the non-encapsulated drug removed, and viability assays were performed by incubating them with HeLa cells. Fig. 6A shows a representative image of HeLa cell growth in RPMI medium with liposomes without MTX, while Fig. 6B shows engineered liposomes containing MTX that have been added to the cells at a final concentration of 3×10^{-7} M in the culture medium and incubated for 72 h. This resulted in an 80 % suppression of cell viability after 5 days as compared with the negative control (Fig. 6C), which corresponded to cell growth without liposomes or any agent. As an additional control, a MTX solution at the same concentration as the one used in the preparation of liposomes was subjected to gel filtration and the eluate added to the cells. As shown in Fig. 6D, cell viability was 75 % of the control, demonstrating that free MTX was mostly retained by the column and thus the effects observed in Fig. 6B can be positively attributed to the encapsulated MTX.

5. Discussion

In this study, we investigated the interaction between engineered liposomes with a specific lipid composition and HeLa cells. Flow cytometry evidenced that the liposomes whose lipid composition had been established in a previous study, POPC:CHOL:DOTAP (0.65:0.15:0.20, mol/mol/mol) [14] interacted with HeLa cells being adsorbed and/or fused with the lipid membrane or internalized into the cell by physiological mechanisms. Note that the amount of CHOL present was sufficient to prevent the gel-to-liquid-crystalline phase transition of the three-component mixture, since DOTAP presented a transition temperature of < 5 ºC [25], close to the one shown by POPC [26]. On the one hand, this CHOL content means that the liposome bilayer does not present cooperativity against external stimuli, becoming resilient to external changes in temperature, pH, and ionic strength. On the other hand, the predominant fluidity of this lipid mixture [16] becomes a key parameter for membrane fusion has been earlier reported [27].

As it is well known, the presence of positively-charged lipids such as DOTAP enhanced the fusion process with the cytoplasmic membrane thanks to electrostatic interaction between the positive charge brought by DOTAP and the negative charge exposed by the plasma membrane because of the presence of several phospholipids (i.e. phosphatidylglycerol, phosphatidylserine or phosphatidylinositol lipids [28]). All these

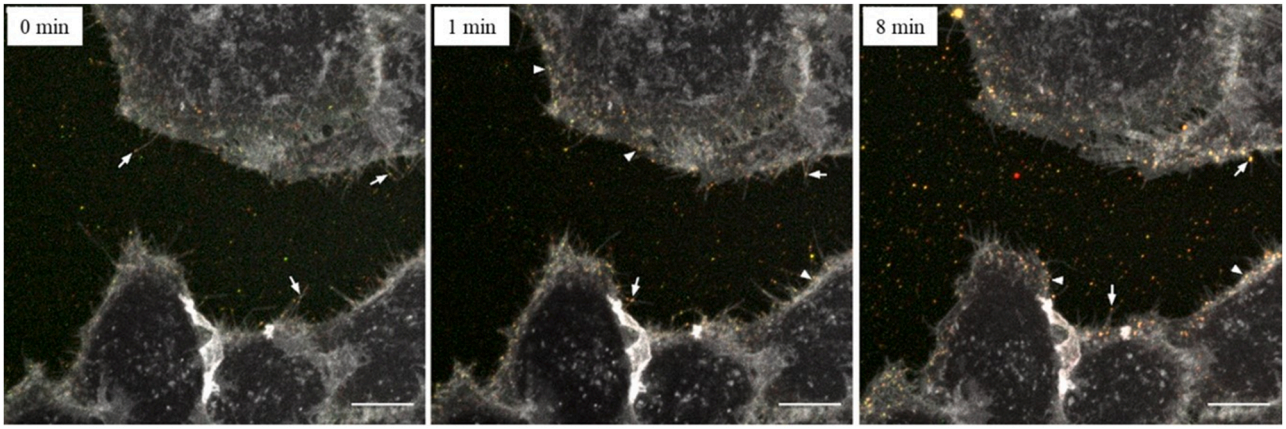

Fig. 4. Liposome-membrane interaction with HeLa cells. Maximum intensity projection of 9 confocal planes (0.369 step size) from the basal side of the cell and at different time points showing calcein staining (green), rhodamine (red) and membranes (gray). Arrows point out liposomes attached to the filopodia, and arrowheads point out liposomes at the cell membrane. Scale bar: 10 μm. Images extracted from supplementary video.

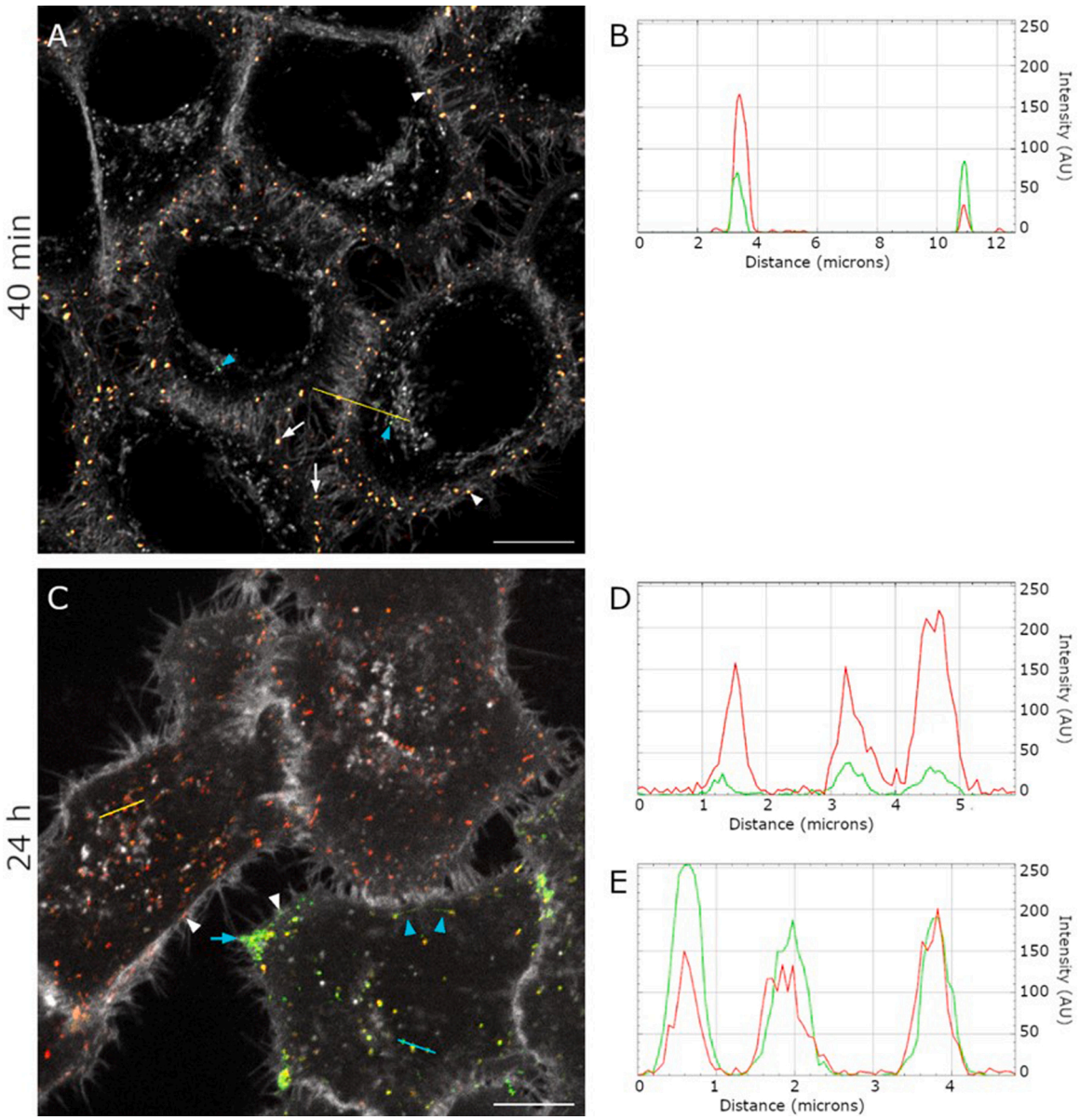

Fig. 5. Liposome localization after 40 min (A, B) and 24 h (C, D, E) of incubation with HeLa cells. Calcein staining is shown in green, rhodamine in red and membranes in grey. Scale bars: 10 μm. (A, C) Single confocal planes. Cyan arrowheads point out internalized liposomes, white arrowheads point out liposomes at the cell membrane, white arrows point out liposomes attached to filopodia, and cyan arrows point out a leading-edge protrusion. (B) Intensity plot of yellow line in A. (D) and (E) Intensity plots of yellow and cyan lines in C, respectively.

properties suggest that the lipid composition of the previously characterized liposomes renders them positively fusogenic candidates with the capacity for drug delivery into HeLa cells.

Flow cytometry indicated that the liposomes were within the cells. However, to obtain further insight into the HeLa cell-liposome interaction and the possible internalization mechanisms we leveraged the complementarity of AFM and CM [29,30]. The features and nanomechanical properties of the HeLa cells identified here using AFM compare well with previously published studies [31–33]. However, here we were interested in the effect exerted by the liposome's lipid composition on Young's modulus and adhesion forces of the cell and how these magnitudes might be related to the interaction and the internalization of liposomes into the HeLa cells. If liposomes fused or partially become inserted in the cell plasma membrane the Young's modulus value should change. Conversely, if liposomes were endocytosed and become internalized no significant changes should be found in the Young's modulus value.

We analyzed the Young's modulus values in the central part of the HeLa cell before and after interaction with the engineered liposomes. Although with our experiments we cannot distinguish between the contribution from the cytoskeleton or the lipid cell membrane, and assuming that nanomechanical properties contain a dominant component originating from actin filaments, the short incubation time and the nature of the liposomes suggested that cytoskeleton structure should be slightly modified, and the differences observed could be due mainly to the interaction of liposomes with the lipid membrane. A clear rigidification (higher mean Young's modulus value) was detected after incorporation of the liposomes, probably due to their partial or total integration in the cell lipid membrane. This rigidification was expected given the relatively high proportion of CHOL present in the engineered liposomes. This is a well-known behavior [34] and we have now confirmed it when liposomes mimicking the HeLa lipid bilayer were integrated using the RBIR method [14]. However, although AFM has evolved as a conventional technique to obtain physicochemical

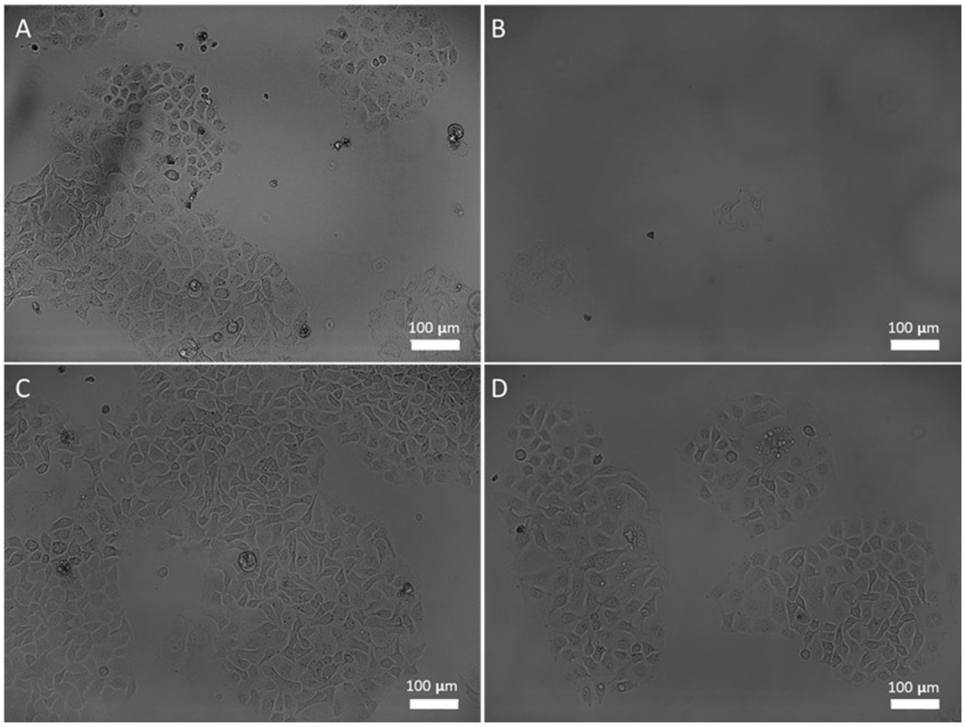

Fig. 6. Growth of HeLa cells under different treatments. Representative pictures of HeLa cells after 72 h of incubation with: A) blank engineered liposomes; B) MTX loaded engineered liposomes; C) without any liposomes or other agents (control); D) free MTX upon filtered through a Sephadex G50 column.

properties at nanoscopic level, it yields insufficient information to discriminate the composition of the structures studied, i.e., lateral segregated lipid domains. At this point, we exploited visualization by CM, with the objective of inspecting the mechanisms underlying the interaction between the liposomes and the HeLa cells.

Confocal observations evidenced the rapid interaction of liposomes with cells following their incorporation into the media. Interestingly, the filopodia of the cells actively contributed to the movement of liposomes towards the membranes, probably the reduced size of the liposomes used enhanced this behaviour. Wider liposomes may be too massive/large for filopodia to capture and carry to the membrane. Filopodia are actin-rich plasma-membrane projections with high dynamic movement which facilitate the cells to scan and interact with the extracellular environment. Several studies have described different cell recruitment mechanisms related with the filopodia to facilitate for instance the entrance of virus [35] or exosomes [36]. Some of the reported mechanisms, such as surfing on filopodia or filopodia grabbing were also observed in the present study with liposomes (see video in Supplementing Material SV1). Of note, bearing in mind that the liposomes were labeled with two fluorescent dyes (PE-Rh at the lipid membrane and calcein at a self-quenching concentration inside the inner aqueous space of the liposome) we observed that the red fluorescence of liposomes before their interaction with the cells evolved into an orange fluorescence signal when captured. This orange color was the superposition of the red fluorescence of the Rh-PE and the green fluorescence of the calcein when released from the liposome into a wider region.

After 40 min, most of the liposomes were near the cell membrane layer and emitted orange fluorescence, indicating fairly rapid calcein release when interacting with the cell membrane and/or the filopodia. Interestingly, liposomes observed inside the cells showed high green fluorescence indicating a complete release of the calcein. After 24 h, most of the liposomes were observed inside the cells, confirming internalization of the liposomes into the HeLa cell cytoplasm. Most of these internalized liposomes emitted a red fluorescence signal (Rh-PE), with almost no green fluorescence (calcein signal), suggesting that the molecule had been released, and that after 24 h of incubation it was diluted or metabolized by the cellular machinery. Strikingly, we observed some HeLa cells where internalized liposomes were emitting high green fluorescence signal suggesting a delayed liposome-membrane interaction process. This delayed interaction between liposomes and cells could be due to the possibility that those cells experienced mitosis and the new cells adhered to the extracellular matrix where liposomes could be deposited non-specifically. In the first minutes of incubation with liposomes, CM revealed that liposomes firstly adhered to the membranes of the cells, but some liposomes were also present at the extracellular matrix between cells. This suggests that although many liposomes interacted with the cell, there was a nearby reservoir of liposomes that only entered later upon cell contact. Note an accumulation of liposomes with strong green fluorescence at cellular protrusion edges, indicating a high internalization of liposomes that remained attached to the surface while the cell was moving towards that direction.

Lastly, we tested the viability of the engineered liposomes carrying MTX as a drug- delivery system, demonstrating the efficient release of MTX after 5 days and thus evidencing the usefulness of the engineered liposomes as a drug- delivery system. Conversely, unloaded liposomes did not affect the viability of the HeLa cells, and the eluted solvent containing possible traces of the drug showed minimal effects on cell viability.

All the data obtained confirm that the POPC:CHOL:DOTAP (0.65:0.15:0.20, mol/mol/mol) liposomes represent a suitable composition for use as a drug nanocarriers against HeLa cells. On the one hand, the interaction between liposomes and cell was enhanced by filopodia capture, opening new perspectives for the release of liposome content through actin rich filopodia. On the other hand, as part of filopodia activity, at the membrane level we have confirmed the fusion mechanism between the engineered liposomes and the cells as previously observed in model membranes. Hence, the determination of changes in nanomechanical properties, such as Young's modulus or adhesion forces in HeLa cells, has proved a practical tool to evidence the incorporation of liposomes within the cell membrane and to test the suitability of a lipid liposome formulation for drug delivery. It is important to consider here

that AFM Young's modulus analysis performed in the present work don't discriminate if rigidification of the cell is only due to the fusion of liposomes with the lipid membrane or if cytoskeleton structure could modulate the effect. More studies with different cell lines should be undertaken in the future to bring some light on the role of cytoskeleton in liposome drug delivery.

6. Conclusion

In this study, AFM and CM evidenced the presence of POPC:CHOL:DOTAP (0.65:0.15:0.20, mol/mol/mol) engineered liposomes, or at least part of the material forming the liposomes, at the cell membrane and internalized in the cytoplasm. The rigidification of the cell membrane after liposome incorporation corroborated the behavior found when the liposomes interacted with lipid model membranes mimicking the HeLa lipid composition. This effect should be studied and verified with other cell lines due to the singular nature of HeLa cells.

We observed that filopodia played an important role in capturing liposomes and bringing them into the cell's membrane body, may be due to the reduced size of the liposomes used. Filopodia from motile cells should be taken into consideration beyond the spontaneous deposition of the liposomes onto the cell membrane when engineering drug delivery systems.

We found that POPC:CHOL:DOTAP engineered liposomes are capable of encapsulating and later releasing MTX. Hence, all results suggest they can be considered as potential drug carriers.

The present paper is a culmination of previously published papers aimed to correlate biophysical experiments with liposomes mimicking HeLa lipid membrane composition with experiments using living HeLa cells. While the results of this work are somehow valuable, some limitations need to be taken in account, only one cell line has been tested and the behavior of the liposomes could be possible to be extrapolated to other cell lines due to the charges on their membranes, a slower interaction rate could be more than possible due to the absence of filopodia in other cell lines. Although the conclusions come from this cell model, the rationale behind the experiments may be of interest when working with other lipid compositions and cell lines.

CRediT authorship contribution statement

Adrià Botet-Carreras: Formal analysis, Writing – original draft. **Manel Bosch Marimon:** Writing – review & editing. **Ruben Millan-Solsona:** Formal analysis. **E. Aubets:** Formal analysis **C.J. Ciudad:** Conceptualization, Visualization, Writing – review & editing. **V. Noè:** Conceptualization, Visualization. **M. Teresa Montero:** Conceptualization, Visualization, Writing – review & editing. **Òscar Domènech:** Formal analysis, Supervision, Writing – review & editing. **Jordi H. Borrell:** Conceptualization, Supervision, Writing – review & editing.

Declaration of Competing Interest

The authors declare that they have no known competing financial interests or personal relationships that could have appeared to influence the work reported in this paper.

Data Availability

No data was used for the research described in the article.

Acknowledgements

This study was supported by the Spanish Ministry of Economy and Competitiveness (PID2019-110210GB-I00), Plan Nacional de Investigación Científica (RTI2018-093901-B-I00) and the Catalan Government (Generalitat de Catalunya) (2014SGR 1442, 2017SGR 94).

Appendix A. Supporting information

Supplementary data associated with this article can be found in the online version at doi:10.1016/j.colsurfb.2022.112968.

References

[1] D.J.A. Crommelin, P. van Hoogevest, G. Storm, The role of liposomes in clinical nanomedicine development. What now? Now what? J. Control. Release 318 (2020) 256–263.
[2] M. Rahman, S. Beg, A. Verma, I. Kazmi, F.J. Ahmed, V. Kumar, F. Anwar, S. Akhter, Liposomes as anticancer therapeutic drug carrier's systems: more than a Tour de Force, Curr. Nanomed. 10 (2020) 178–185.
[3] Y. Okumura, M. Yamauchi, M. Yamamoto, J. Sunamoto, Interaction of a Fusogenic Liposome with HeLa Cell, Proc. Jpn. Acad. Ser. B. 69 (1993) 45–50.
[4] M.L. Immordino, F. Dosio, L. Cattel, Stealth liposomes: review of the basic science, rationale, and clinical applications, existing and potential, Int. J. Nanomed. 1 (2006) 297–315.
[5] D.J. A Crommelin, G.W. Bos, G. Storm, 2002. Liposomes-successful carrier systems for targeted drug delivery, Drug Delivery parnerships news, 2 (101).
[6] C. Noé, J. Hernandez-Borrell, S.C. Kinsky, E. Matsuura, L. Leserman, Inhibition of cell proliferation with antibody-targeted liposomes containing methotrexate-γ-dimyristoylphosphatidylethanolamine, Biochim. Biophys. Acta - Biomembr. 946 (1988) 253–260.
[7] J. Hernández-Borrell, A new confirmation of selective action of liposomes, Int. J. Pharm. (1988).
[8] M. Li, C. Du, N. Guo, Y. Teng, X. Meng, H. Sun, S. Li, P. Yu, H. Galons, Composition design and medical application of liposomes, Eur. J. Med. Chem. 164 (2019) 640–653.
[9] S. Singh, P. Chaturvedi, A. Singh, S.K. Jain, Clinical approved liposomal formulations: an over view, J. Emerg. Technol. Innov. Res. 8 (2021) 856–868.
[10] M.A. Busquets, J. Estelrich, Prussian blue nanoparticles: synthesis, surface modification, and biomedical applications, Drug Discov. Today 25 (2020) 1431–1443.
[11] N. Düzgüneş, S. Nir, Mechanisms and kinetics of liposome–cell interactions, Adv. Drug Deliv. Rev. 40 (1999) 3–18.
[12] S.-T. Yang, A.J.B. Kreutzberger, J. Lee, V. Kiessling, L.K. Tamm, The role of cholesterol in membrane fusion, Chem. Phys. Lipids 199 (2016) 136–143.
[13] T.L. Andresen, J.B. Larsen, Compositional inhomogeneity of drug delivery liposomes quantified at the single liposome level, Acta Biomater. 118 (2020) 207–214.
[14] A. Botet-Carreras, M.T. Montero, J. Sot, Ò. Domènech, J.H. Borrell, Characterization of monolayers and liposomes that mimic lipid composition of HeLa cells, Colloids Surf. B Biointerfaces 196 (2020), 111288.
[15] R. Blumenthal, M.J. Clague, S.R. Durell, R.M. Epand, Membrane fusion, Chem. Rev. 103 (2003) 53–69.
[16] A. Botet-Carreras, M.T. Montero, J. Sot, Ò. Domènech, J.H. Borrell, Engineering and development of model lipid membranes mimicking the HeLa cell membrane, Colloids Surf. A Physicochem. Eng. Asp. 630 (2021), 127663.
[17] C. Suárez-Germà, L.M.S. Loura, M. Prieto, Ò. Domènech, M.T. Montero, A. Rodríguez-Banqueri, J.L. Vázquez-Ibar, J. Hernández-Borrell, Membrane protein–lipid selectivity: enhancing sensitivity for modeling FRET data, J. Phys. Chem. B. 116 (2012) 2438–2445.
[18] S. Dutta, B. Watson, S. Mattoo, J. Rochet, Calcein release assay to measure membrane permeabilization by recombinant alpha-synuclein, Bio-Protoc. 10 (2020).
[19] J.J. Roa, G. Oncins, J. Diaz, F. Sanz, M. Segarra, Calculation of Young's modulus value by means of AFM, Recent Pat. Nanotechnol. 5 (2011) 27–36.
[20] S.E. Cross, Y.-S. Jin, J. Rao, J.K. Gimzewski, Nanomechanical analysis of cells from cancer patients, Nat. Nanotechnol. 2 (2007) 780–783.
[21] K. Pogoda, J. Jaczewska, J. Wiltowska-Zuber, O. Klymenko, K. Zuber, M. Fornal, M. Lekka, Depth-sensing analysis of cytoskeleton organization based on AFM data, Eur. Biophys. J. 41 (2012) 79–87.
[22] M. Radmacher, Studying the mechanics of cellular processes by atomic force microscopy, Methods Cell Biol. (2007) 347–372.
[23] J. Schindelin, I. Arganda-Carreras, E. Frise, V. Kaynig, M. Longair, T. Pietzsch, S. Preibisch, C. Rueden, S. Saalfeld, B. Schmid, J.-Y. Tinevez, D.J. White, V. Hartenstein, K. Eliceiri, P. Tomancak, A. Cardona, Fiji: an open-source platform for biological-image analysis, Nat. Methods 9 (2012) 676–682.
[24] T. Ferreira, K. Miura, B. Chef, 2015. J. Eglinger, Zenodo (2015) Scripts: BAR 1.1.6 (Version 1.1.6).
[25] A.E. Regelin, S. Fankhaenel, L. Gürtesch, C. Prinz, G. von Kiedrowski, U. Massing, Biophysical and lipofection studies of DOTAP analogs, Biochim. Biophys. Acta - Biomembr. 1464 (2000) 151–164.
[26] J. Hernandez-Borrell, K.M.W. Keough, Heteroacid phosphatidylcholines with different amounts of unsaturation respond differently to cholesterol, Biochim. Biophys. Acta - Biomembr. 1153 (1993) 277–282.
[27] J. Bompard, A. Rosso, L. Brizuela, S. Mebarek, L.J. Blum, A.-M. Trunfio-Sfarghiu, G. Lollo, T. Granjon, A. Girard-Egrot, O. Maniti, Membrane fluidity as a new means to selectively target cancer cells with fusogenic lipid carriers, Langmuir 36 (2020) 5134–5144.
[28] K. Stebelska, P. Wyrozumska, J. Gubernator, A. Sikorski, Higly fusogenic cationic liposomes transiently permeabilize the plasma membrane of HeLa cells, Cell. Mol. Biol. Lett. 12 (2007).

[29] C.A.J. Putman, A.M. van Leeuwen, B.G. de Grooth, K. Rado??ević, K.O. van der Werf, N.F. Van Hulst, J. Greve, Atomic force microscopy combined with confocal laser scanning microscopy: a new look at cells, Bioimaging 1 (1993) 63–70.
[30] T.F.D. Fernandes, O. Saavedra-Villanueva, E. Margeat, P. Milhiet, L. Costa, Synchronous, crosstalk-free correlative AFM and confocal microscopies/spectroscopies, Sci. Rep. 10 (2020) 7098.
[31] A. Gigler, M. Holzwarth, O. Marti, Local nanomechanical properties of HeLa-cell surfaces, J. Phys. Conf. Ser. 61 (2007) 780–784.
[32] M. Checa, R. Millan-Solsona, A. Glinkowska Mares, S. Pujals, G. Gomila, Dielectric imaging of fixed HeLa cells by in-liquid scanning dielectric force volume microscopy, Nanomaterials 11 (2021) 1402.
[33] K. Hayashi, M. Iwata, Stiffness of cancer cells measured with an AFM indentation method, J. Mech. Behav. Biomed. Mater. 49 (2015) 105–111.
[34] M.D. Houslay, K.K. Stanley, Dynamics of biological membranes, Biochem. Educ. 11 (1983) 157.
[35] K. Chang, J. Baginski, S.F. Hassan, M. Volin, D. Shukla, V. Tiwari, Filopodia and viruses: an analysis of membrane processes in entry mechanisms, Front. Microbiol. 7 (2016) 300.
[36] W. Heusermann, J. Hean, D. Trojer, E. Steib, S. von Bueren, A. Graff-Meyer, C. Genoud, K. Martin, N. Pizzato, J. Voshol, D.V. Morrissey, S.E.L. Andaloussi, M. J. Wood, N.C. Meisner-Kober, Exosomes surf on filopodia to enter cells at endocytic hot spots, traffic within endosomes, and are targeted to the ER, J. Cell Biol. 213 (2016) 173–184.